

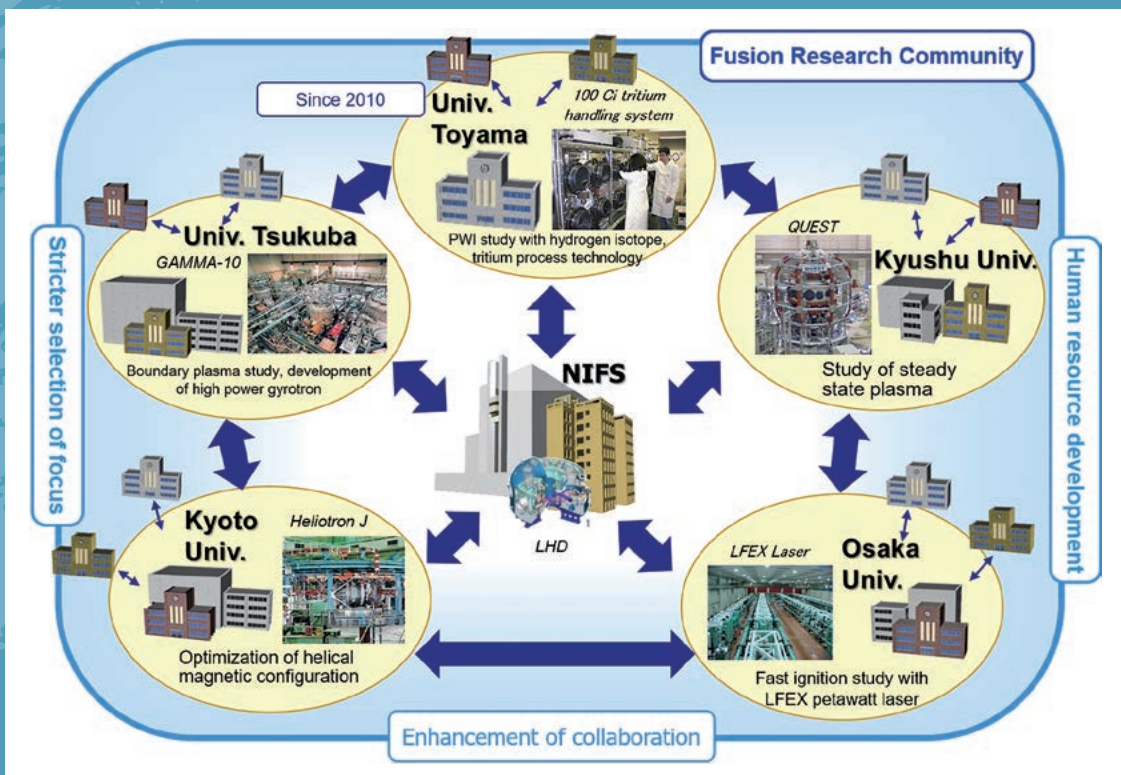
# 8. Bilateral Collaboration Research

The purpose of the Bilateral Collaboration Research Program (BCRP) is to enforce the activities of nuclear fusion research in the universities by using their middle-size experimental facilities of the specific university research centers as the joint-use facilities for all university researchers in Japan. The current program involves five university research centers as follows:

- Plasma Research Center, University of Tsukuba
- Laboratory of Complex Energy Process, Institute of Advanced Energy, Kyoto University
- Institute of Laser Engineering, Osaka University
- Advanced Fusion Research Center, Research Institute for Applied Mechanics, Kyushu University
- Hydrogen Isotope Research Center, University of Toyama

In the BCRP, each research center can have its own collaboration programs, using its main facility. Researchers at other universities can visit the research center and carry out their own collaboration research there, as if the facility belongs to NIFS. That is, all these activities are supported financially by NIFS for the research subjects in the BCRP. The BCRP subjects are subscribed to from all over Japan every year as one of the four frameworks of the NIFS collaboration program. The collaboration research committee, which is organized under the administrative board of NIFS, examines and selects the subjects.

(S. Sakakibara)



## University of Tsukuba



Fig. 1. Bird's eye view of GAMMA 10/PDX.

## Highlight

## Study of boundary plasmas by making use of open magnetic field configuration and development in high power gyrotrons towards the DEMO project

In the Plasma Research Center, University of Tsukuba, studies of boundary plasma and development of high-power gyrotrons have been performed under a bilateral collaboration research program. The GAMMA 10/PDX (Fig. 1) is the world's largest tandem mirror device with many plasma production/heating devices. A divertor simulation study has been intensively promoted by using a divertor simulation experimental module (D-module), shown at the lower left of Fig. 1. Nitrogen Molecular Assisted/Activated Recombination (N-MAR) processes have been investigated by combination seeding of  $N_2$  and  $H_2$ , which leads to a clear decrease of ion flux to the divertor target. In the case of  $N_2$  seeding, the emission intensity ratio of  $H_\alpha/H_\beta$  does not increase, unlike the case of  $H_2$  or Ne seeding, indicating dominant recombination process changes from Hydrogen-MAR (H-MAR) to N-MAR. A test of a new 28/35 GHz dual-frequency gyrotron has been carried out. The new linear plasma device with superconducting coils has been constructed to contribute to the DEMO divertor design.

Remarkable progress has been made on understanding the role of  $N_2$  and  $H_2$  seeding on plasma detachment in divertor simulation experiments, using the end-loss region of GAMMA 10/PDX. These issues have been experimentally studied for different gas species, seeding rate and target angles. We have investigated Nitrogen Molecular Assisted/Activated Recombination (N-MAR) processes during combination seeding of  $N_2$  and  $H_2$ , which led to a clear decrease of ion flux to the divertor target. In the case of  $N_2$  seeding, the emission intensity ratio of  $H_\alpha/H_\beta$  does not increase, unlike cases of  $H_2$  or Ne seeding. These indicate dominant recombination process changes from Hydrogen-MAR (H-MAR) to N-MAR. Spatial profiles of  $N_2$  emission observed by a high-speed camera with a band-pass filter show that  $N_2$  emission was initially strong near the corner of the V-shaped target, and then it became weaker with increasing  $H_2$  pressure. This indicates that  $N_2$  was consumed by N-MAR. Concerning target configuration, the V-shaped target experiment at different target angles shows that an area of H-MAR moved upstream in the case of a small angle slot. It is important to measure the plasma density and temperature at the center part of the V-shaped target. We plan detailed measurements by microwave interferometer and Thomson scattering in the region.

As for the advanced diagnostic development, a Ku-band (12-18 GHz) multichannel Doppler reflectometer (DR) and a multi-pass Thomson scattering (TS) system at the end region have progressed. The former system has been developed in the GAMMA 10/PDX tandem mirror to improve the applicability of DR measurement for simultaneous monitoring of turbulent flows at different radial locations. In this fiscal year, the previous single-channel DR circuit was replaced by a multichannel microwave system using a nonlinear transmission line (NLTL) based combgenerator with the heterodyne technique. An initial result of the application to GAMMA 10/PDX central cell plasma was obtained and it showed clear Doppler frequency shifts during an additional ion cyclotron resonance frequency (ICRF) heating and gas-puffing experiment. In order to improve the signal intensity of the Thomson scattering (TS) system in the end region, we have been developing a multi-pass system in the end-TS system. The double-pass TS system was constructed by adding a lens and a reflection mirror for the image transfer optical system, leading to an increase in TS scattering signals. We plan to develop the multi-pass TS system by adding a laser polarization control system.

A new 154/116 GHz dual-frequency gyrotron and 28 GHz gyrotron have been developed for LHD and QUEST, respectively. The Output power of 1.66 MW and 1.34 MW has been achieved at oscillation frequencies of 154.05 GHz and 116.15 GHz, respectively. At the experimental test of a new 28 GHz gyrotron, the output power of 1.24 MW at an oscillation frequency of 28.06 GHz has been achieved. A maximum total efficiency of 53.1% has been obtained with collector potential depression (CPD). Both gyrotrons were also confirmed to be problem-free in also other property tests.

In order to further promote divertor simulation study, a new linear plasma device Pilot GAMMA PDX-SC (Fig. 2) has been constructed. A pair of NbTi superconducting coils with a bore of 0.9m and a pair of Cu coils with one of  $\sim 1.5$  m were utilized to produce a simple mirror configuration. The maximum magnetic field was 1.5 T and the mirror ratio was 20~30. The superconducting coils, Cu coils and the vacuum vessel have already been constructed and installed. The target plasma parameters are the following: plasma density  $10^{19} \text{ m}^{-3}$ , electron and ion temperatures several tens of eV and a discharge duration of 10~100 s. A biased limiter and biased segmented plates will be used to suppress MHD instability. Hot cathode plasma discharge with  $LaB_6$  and helicon plasma discharge have been developed as a steady state plasma source. The first plasma is expected in 2022.

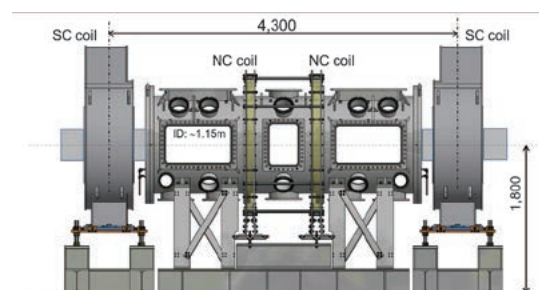


Fig. 2 Schematic view of Pilot GAMMA PDX-SC.

(M. Sakamoto)



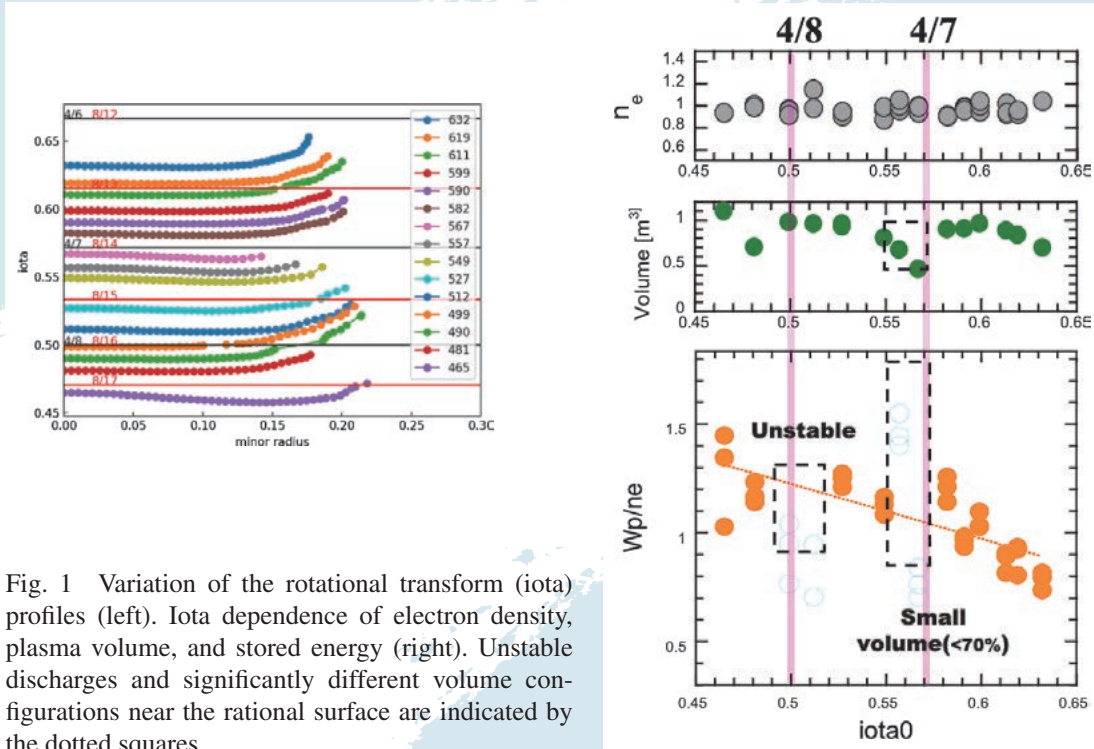


Fig. 1 Variation of the rotational transform (iota) profiles (left). Iota dependence of electron density, plasma volume, and stored energy (right). Unstable discharges and significantly different volume configurations near the rational surface are indicated by the dotted squares.

Highlight

## Iota dependence of the confinement properties in Heliotron J

The Heliotron J device features a wide flexibility of configuration control. So far, the effect of the bumpiness component (toroidal mirror ratio) in the magnetic field spectrum on neoclassical transport, MHD, and fast ion confinement has been investigated as a key control knob for configuration optimization. We have recently attempted to extend the parameter spaces characterizing magnetic field configuration and focused on rotational transformation (iota) control experiments this year.

The iota profile can be modified by controlling the current ratio between the toroidal and helical coils in the Heliotron J. In this experiment, the iota profile with low magnetic shear varied widely from 0.46 to 0.63, while keeping a line-averaged density at about  $1 \times 10^{19} \text{ m}^{-3}$ . The magnetic field strength was adjusted so that the power deposition of the electron cyclotron heating (ECH) was kept at the plasma center.

As shown in Fig. 1, the energy confinement degraded with increasing the rotational transform, as a general tendency. Note that some data was excluded from the analysis because the plasma conditions were not regarded as stable, as indicated by the dotted square. The unstable discharges were observed at the iota near the low-order rational surfaces.

A comparison between the stored energy and the effective helical ripple ( $\epsilon_{\text{eff}}$ ) calculated with the MCviewer code shows an unclear dependence of the stored energy on the helical ripple. This result is different from that of the LHD, where improved neoclassical transport in the lower  $\epsilon_{\text{eff}}$  configuration accompanies a reduction of turbulence transport through enhanced zonal flow activity. In the Heliotron J case, in contrast, the rotational transform seems to relate more directly to the turbulent suppression. This study is still ongoing, based on a comparison with a numerical study of turbulence transport.

## Research Topics from Bilateral Collaboration Program in Heliotron J

The main objectives of the research in the Heliotron J device under this Bilateral Collaboration Program are to experimentally and theoretically investigate the transport and stability of fusion plasmas in an advanced helical field and to improve the plasma performance through advanced helical-field control. Picked up in FY2021 are the following five key topics; (1) plasma structure formation control and plasma transport improvement by magnetic field configuration control, (2) spatial distribution, flow, and current control for confinement improvement, (3) clarification and control of plasma fluctuation structure formation in the core and peripheral regions, (4) characterization and control of energetic-particle-driven MHD instabilities, and (5) optimization of particle fueling and heating scenarios. Nineteen projects, including our baseline one, were adopted. High magnetic field experiments were conducted for about five months, from September to the beginning of February.

### Characterization of small-pellet ablation cloud

In recent years, diagnostic systems for the pellet ablation cloud have progressed at the Heliotron J. A low-speed ( $260 \pm 30 \text{ m s}^{-1}$ ) and small-size (1.1 – 1.2 mm) pellet injection enabled a high-density operation even in the middle-size device. Visible imaging, the emission of which is dominated by the bright Balmer- $\beta$  line, using a high-speed camera, observed a fluctuation surrounding the ablation cloud that rotated around the magnetic field line. The relative fluctuation level went up to about 15%, suggesting that this phenomenon was induced by the ablation process. For the measurement of the ablation cloud density, fast-imaging spectroscopy for the Balmer- $\beta$  line at 486.135 nm has been developed. We found that conventional filter spectroscopy, based on the intensity ratio of Balmer- $\beta$  between band-pass filters having different pass-band widths, was not applicable because the Stark-broadening was too small for our density regime. The newly applied near-infrared Paschen- $\alpha$  line supports this observation at 1875.13 nm, which has a broader Stark-width than Balmer- $\beta$  for the same density.

### Free-boundary simulation of energetic-particle driven modes in Heliotron J

The confinement of fusion-produced energetic particles (EP) is essential for achieving self-sustainable fusion plasmas. However, EP-driven MHD instabilities can be enhanced by the resonant interaction between EPs and shear Alfvén waves (SAW) during the slowing-down process. A computational simulation is an effective tool for investigating the linear and nonlinear interactions between the EPs and the MHD waves, such as SAW, in 3-dimensional plasma. To this end, a particle-MHD hybrid simulation code, MEGA, has been implemented in the Heliotron J. In the early research phase, the MEGA code failed to reproduce the low- $n$  EP-driven MHD modes observed in the Heliotron J experiments. We solved this problem by extending the code to one with a free boundary condition. This enabled analysis on the clarification of the EP-SAW interactions, including frequency chirping, EP transport, and the mitigation of EP-driven MHD instability, which are useful in promoting our further collaboration research from the viewpoint of both theory and experiment.

Many research topics have made progress with collaborative researchers under the Bilateral Collaboration Program in the Heliotron J project, such as (i) electromagnetic wave measurements, such as multi-line-of-sight interferometry and multi-channel reflectometry, (ii) spectroscopic diagnostics, such as high sensitivity beam emission spectroscopy for local turbulent fluctuation measurements, and fast Stark spectroscopy for pellet ablation clouds, (iii) measurement of peripheral plasma flow and heat flux, and (iv) active diagnostics, such as multi-pass Thomson scattering measurements, event-triggered Thomson scattering and laser blow-off spectroscopy are progressing.

(K. Nagasaki)

## Study of Fast Ignition Scheme of Laser fusion with Extremely High-density plasmas

We have performed fundamental research into laser fusion, especially the fast ignition scheme, which enables us to separate the laser fusion process into three phases, i.e., compression, heating, and burning, using the GEKKO XII and LFEX laser systems at the Institute of Laser Engineering, Osaka University. The research included target fabrication, laser development, laser experiments, simulations, and reactor technology development. In FY2021, the following progress was made through the Bilateral Collaboration Research Program with NIFS and other collaborators from universities and institutes (NIFS12KUGK057 as the base project).

### Compression of Solid Ball Target

For the fast ignition of laser fusion, we do not need to apply heat in the implosion phase, which means that high implosion velocity is not required, so we can adapt a solid ball target instead of one of thin shell. A solid ball implosion is more robust than a shell implosion from reducing hydro-instabilities. However, to achieve a high-density core, the temporal pulse profile of an implosion laser must be controlled precisely to deliver multiple shocks arriving at the same time at the center. In the experiment of FY2021, intensities of the GEKKO XII laser were increased in three steps by following the optimal pulse profile obtained by a hydrodynamics simulation, PINOCO. Although the pulse profile was set up in three-steps as expected, the outputs of twelve laser beams were not kept stable and thus the core density could not be as high as predicted by PINOCO. We are planning to maintain the laser output of the GEKKO XII in the next fiscal year.

### Target Fabrication

In laser fusion, solid tritium (T) and deuterium (D) are used as fuel in the form of a spherical solid with a medium shell. High sphericity and uniformity of the shell thickness are required for these fuels. Optical inspection is an effective method, but thickness measurement with an accuracy of  $0.1\mu\text{m}$  is required. However, due to the difficulty of handling gaseous radioactive materials in the standard state, the refractive indices of solid T<sub>2</sub> are only estimated values and have not been measured. In FY2021 we solidified DT in a wedge-shaped cell at temperatures below 19 K, and measured the temperature dependence of the refractive index through a laser at a wavelength of 546 nm. This is the first new physical property of T<sub>2</sub> measured in about 60 years. Thus it is an important result that will be useful for fuel inspection in future fusion reactors.

### Simulation Research of Compression, Heating, and Ignition

It was confirmed that 1.3 MJ (gain 0.7) of neutrons were produced in response to 1.8 MJ of laser energy input in the NIF experiment at Lawrence Livermore Laboratory in the United States, and that the shell target, which was imploded by the indirect irradiation method, was compressed several thousand times and fusion burning was started. Future

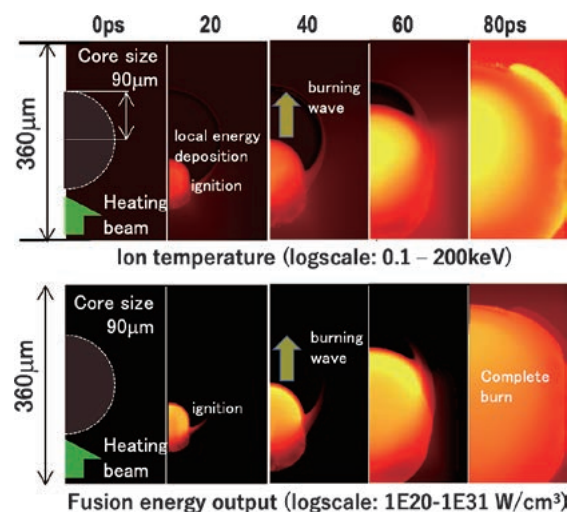


Fig. 1 The required parameters; implosion laser 380 kJ, density of core 500 g/cc, core radius 90 µm, core internal energy 20 kJ, heating laser 200 kJ/30ps (2ω), intensity  $3 \times 10^{20}$  W/cm<sup>2</sup>, coupling efficiency 20% (40 kJ to the core).

development will be necessary to establish a high-gain laser fusion design and the identification and solution of elemental problems to realize it. We have designed a high-gain laser fusion (gain x130) by the FIBMET code.

### **Improvement of GXII and LFEX laser system**

The electrical control system of the GXII laser system has not been changed much since its construction and has become obsolete, so a complete review is underway. The trigger signal system is also synchronized with the LFEX laser system, so a complete renovation plan has been prepared and the equipment is gradually being replaced. The monitor system is also under review, and a replacement plan for the energy measurement system has been prepared and will be tested on one beam. We have also developed and tested software for the networking of the beam pattern monitors in the amplification section.

For the LFEX laser system, the alignment laser was replaced with a broadband fiber laser to suppress interference in the beam pattern monitor and improve visibility of the intensity distribution. This has greatly improved the detection accuracy of damage to optical elements and beam kicking. In addition, stray light at the compressor, which could not be detected by alignment lasers, can be now, and countermeasures taken. In the oscillator section, the OPCPA amplification region was completely revised in order to stabilize the seed light, and the design was made to reduce the overall gain by fiberization and OPCPA.

(R. Kodama, H. Shiraga, S. Fujioka, K. Yamanoi, Y. Sentoku, and J. Kawanaka)



## Research activities on QUEST in FY2021

We will summarize the activities on the Advanced Fusion Research Center, the Research Institute for Applied Mechanics in Kyushu University during April 2021 – March 2022. The QUEST experiments were executed during 30th Jun. – 12th Aug. (2021 Spring/Summer, shot no. 45927–46319) and 7th Sep. – 18th Mar. (2021 Autumn/Winter, shot no. 46320–48675). The main topics of the QUEST experiments in FY2019 are listed below.

- 1) An operation of approximately 673K was carried out and strong fuel particle retention was subdued. The pulse duration at the wall temperature was limited to 40 m, due to wall saturation. Water-cooling of the hot wall had been applied and the pulse duration could be extended to about 4 h. The wall saturation could be avoided during the water-cooling phase, but suffered a reoccurrence when the water-cooling was off.
- 2) Co-axial helicity injection (CHI) was applied to achieve an efficient plasma start-up. Improvement of a gas-injection system for CHI worked well and electron density of  $6 \times 10^{19} \text{ m}^{-3}$  could be achieved at an optimized condition of CHI.
- 3) To realize a double swing of center solenoid current safely, even if the current monitor does not work, the high-speed interlock circuit has been improved so as to mask the switching command in preset time. A plasma current dip during the dead time was decreased and a plasma current of 120 kA with peak electron density of  $2.3 \times 10^{18} \text{ m}^{-3}$  has been achieved.
- 4) To study the effect of plasma flow on material transport near the first wall, “directional material probes (DMPs)” were installed. Visual observation revealed that the deposition layers on DMPs were formed with a directionality in a counterclockwise direction in the toroidal direction. Some parts of the deposited layer on a DMP were examined by the glow discharge optical emission spectroscopy (GDOES) in NIFS, and depositions of tungsten, iron, and carbon were observed.
- 5) The original idea for the direct detection of electron Bernstein wave (EBW) was to utilize a 400 GHz 0.1 ms/50 kW gyrotron as a scattering source. We have decided to change the scattering source to a CW/50 mW HCN-laser (890GHz), expecting the 60 dB source power down could be partly compensated for by an effective integration time of detection.
- 6) XPS (X-ray Photoelectron Spectroscopy) analyses showed that the major deposits on the plasma facing wall for the QUEST 2020Spring/Summer campaign were carbon and metal oxide. A thick deposit was observed for the Equator wall, whose thickness was about 20 nm, although that for the top and bottom were around 10 nm. Based on TDS (thermal desorption spectroscopy) results, large hydrogen retention was found for the bottom sample, indicating that most of the hydrogen would be trapped as C-H bonds.
- 7) To double the toroidal field (TF) on QUEST, a module consisting of a Lithium-ion capacitor and a DC-DC buck converter has been designed and developed. The resultant flat-topped-current is 800 A. The wave form in the bench test matches up to the circuit simulation. Assembling the 125 modules in parallel, the coil current reaches 100 kA, and hence the TF is doubled.
- 8) Tokamak start-up simulations for divertor configuration without RF current drive are demonstrated. Using an axisymmetric MHD simulation code, coupled with a conducting vessel and coils, time evolutions of plasma with a small cross-section to a divertor configuration are investigated and compared with experiments.
- 9) We study the driving mechanism of toroidal flow by electron cyclotron heating (ECH) related to the 3-D magnetic field, by experimentally verifying the  $\mathbf{J} \times \mathbf{B}$  torque by ECH and comparing it with the GNET simulation in QUEST. Assuming a QUEST size tokamak plasma (central temperature 100 eV, density  $1.0 \times 10^{18} \text{ m}^{-3}$ ) we have obtained a significant torque by introducing 0.1% toroidal field ripples as a 3-D magnetic field.
- 10) Various waves have been found to emerge in the ion cyclotron range of frequencies to whistler frequencies, in accordance with significant generation of hard X-rays on QUEST. The frequencies of the waves always

chirped in time, even though plasma parameters, which were experimentally measured, were steady for the timescale of their chirps, suggesting rapid evolution of velocity distributions of energetic electrons.

- 11) In order to accurately understand the surface alteration of plasma-facing materials during steady-state discharges and the associated fuel particle absorption, we plan to clarify the depth profiles of hydrogen isotopes and impurities in the samples exposed to steady-state plasma at QUEST. In this fiscal year, 1) the environmental arrangements of the ion beam analyzer and the nuclear reaction analyzer (NRA), and 2) the installation of samples for analysis at QUEST were carried out.
- 12) We have jointly developed a large-capacity database with the Pan-Omics Data-Driven Research Innovation Center of Kyushu University, which can register many types of data and provide them with a unified user interface such as a Jupiter notebook. With this provision, researchers will be able to easily access the data they need, and will be able to perform efficient data analysis, which is expected to further advanced research.
- 13) The potential fluctuation measured by the divertor probes was analyzed in a QUEST divertor configuration. Strong correlation between the fluctuation at different channels was observed. By analyzing the phase delay of each channel, it has been found that the speed of the fluctuation propagation is in the order of several hundred meters per second in a radial direction, and the direction of the propagation changes during the current ramp-up discharges.
- 14) Experiments to model an ECH assisted Ohmic start-up were performed. It was found that breakdown was slower at higher ECH power above 10 kW and a prefill pressure of  $\sim 0.7$  mPa. The result was qualitatively similar to LATE and TST-2. Discharge tuning for an Ohmic start-up was also performed. Closed flux surfaces were successfully obtained with EC preionization at  $\sim 1.5$  mPa.
- 15) A novel divertor biasing using four toroidally-distributed biased plates has been attempted in low density plasmas produced by ECH. Several current filaments along the scrape-off-layer (SOL) have been generated by the divertor biasing. Enhanced losses of non-thermal electrons leading to  $\sim 5\%$  reduction in plasma current, and a noticeable decrease of divertor particle flux have been observed during the biasing. The observed effects are thought to be due to generation of resonant magnetic perturbations produced by the SOL current filaments.
- 16) For the spectroscopic measurements of (i) hydrogen atom density, (ii)  $T_e$  and  $n_e$  (with helium puffing), and (iii)  $Z_{\text{eff}}$  (in high-density discharges), a low-dispersion imaging spectrometer was developed. The spectrometer simultaneously measures 27 spectra in the wavelength range of 400–730 nm with a wavelength resolution of 0.7 nm and a frame rate of up to 23 fps.
- 17) The circuits with vacuum chamber currents with 58 segments, a pair of horizontal coil and plasma have been solved for the vertical plasma position control system in QUEST. For the central value of the n-index of  $-0.069$ , the coil current and voltage required for Ohmic divertor experiments with initial vertical shift of 5.5 cm can be supplied from the power supply system presently being prepared (IHC = 200 A, VHC = 200 V, PHC = 50 kW).

HANADA Kazuaki (Kyushu University) 1), 2)  
 NAKAMURA Kazuo (Kyushu University) 3)  
 MASUZAKI Takashi (NIFS) 4)  
 KUBO Shin (Chubu University) 5)  
 OYA Yasuhisa (Shizuoka University) 6)  
 ONCHI Takumi (Kyushu University) 7)  
 TSUTSUI Hiroaki (Tokyo Institute of Technology) 8)  
 MURAKAMI Sadayoshi (Kyoto University) 9)  
 IKEZOE Ryuya (Kyushu University) 10)

YAJIMA Miyuki (NIFS) 11)  
 HASEGAWA Makoto (Kyushu University) 12)  
 KOBAYASHI Masahiro (NIFS) 13)  
 TSUJII Naoto (University of Tokyo) 14)  
 TOI Kazuo (NIFS) 15)  
 SHIKAMA Taichi (Kyoto University) 16)  
 MITARAI Osamu (Institute for Advanced Fusion and Physics Education) 17)

(K. Hanada)

## University of Toyama

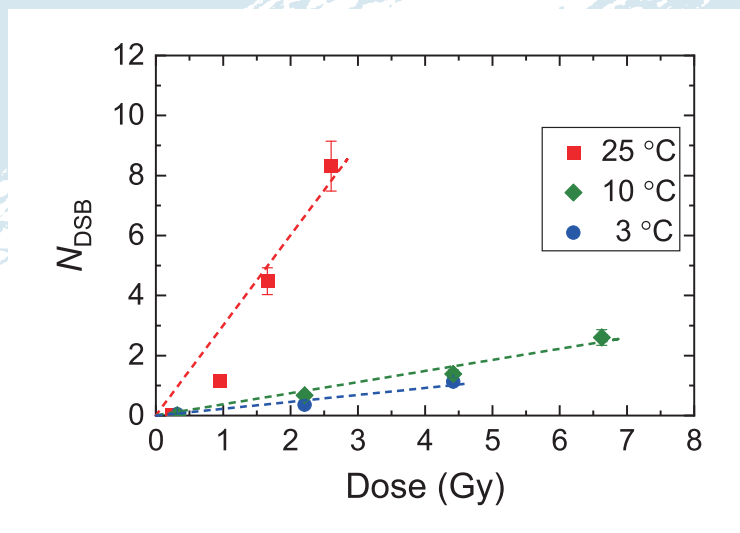


Fig. 1 Number of double-strand breaks,  $N_{\text{DSB}}$ , of genome-sized DNA molecules of T4 GT7 bacteriophage in high concentration tritiated water ( $3\text{--}4\text{ MBq/cm}^3$ ) as a function of  $\beta$ -ray irradiation dose.

## Highlight

## Research Activities in Hydrogen Isotope Research Center, Organization for Promotion of Research, University of Toyama

A simple experimental system to examine the rate of double strand breaks (DSBs) of genome-sized DNA molecules in tritiated water under well-controlled conditions was established for the validation of computer simulation on interactions of biomolecules and ionizing radiation. Radiation-induced DSBs were clearly recognizable at tritium concentrations of  $3\text{--}4\text{ MBq/cm}^3$ , while it was unnoticeable at  $\sim\text{kBq/cm}^3$ . The number of DSBs,  $N_{\text{DSB}}$ , increased proportionally with the irradiation dose, as shown in Fig. 1. The rate of DSBs showed a clear increase with rising water temperature. These observations indicate that irradiation effects and thermal effects are synergistic with each other. One of the possible mechanisms underlying this synergism is that a single strand break (SSB) induced by radiation developed to DSB by thermal effects and vice versa.

*[Double-strand breaks in a genome-sized DNA caused by beta-ray under cellular environment (T. Kenmotsu, Doshisha U.)]*

*Tritium transport in fusion reactor materials* (Y. Hatano, U. Toyama): A nuclear fusion power plant will use a steam turbine to generate electricity. Tritium (T) permeation through steam generator piping results in the risk of uncontrolled T leakage to the environment. Therefore, T permeation must be precisely evaluated and minimized. Nickel alloys are widely used as pipe materials. In this study the permeation of T from/to high temperature, high pressure water through Inconel 600 film was examined.

Thin disks of Inconel 600 were used as samples. The permeation device used was made of type 304 stainless steel and separated into two chambers by a sample disk. The upstream chamber was filled with tritiated water ( $0.9 \text{ MBq/cm}^3$ ) and the downstream side was filled with non-radioactive water. The device was placed in a forced convection oven and heated to  $280^\circ\text{C}$  for 14–60 h. The vapor pressure of water at this temperature was 6.4 MPa. After heating, the downstream chamber was opened and the concentration of T in water was measured using a liquid scintillation counter. Correlation between heating time and the amount of T permeated to the downstream side is shown in Fig. 2. The initial permeation rate up to 14 h was 1 Bq/h. After 14 h, the data points spread in a relatively wide range but the permeation rate on average was 3 Bq/h after 14 h. Namely, the permeation rate increased after 14 h. Here T cannot permeate through the sample in the form of a HTO molecule. T atoms are liberated by the oxidation of metals and a part of the liberated T atoms permeate to the downstream, together with H atoms. The other part of liberated T is released into the upstream chamber as HT. At the downstream side surface, a T atom is released in the form of HTO, via isotope exchange with  $\text{H}_2\text{O}$  or as HT, via recombination with a H atom. Namely, the partial pressure of HT increases with heating time in both chambers. This increase in HT partial pressure is one of the possible reasons for the increase in permeation rate at 14 h.

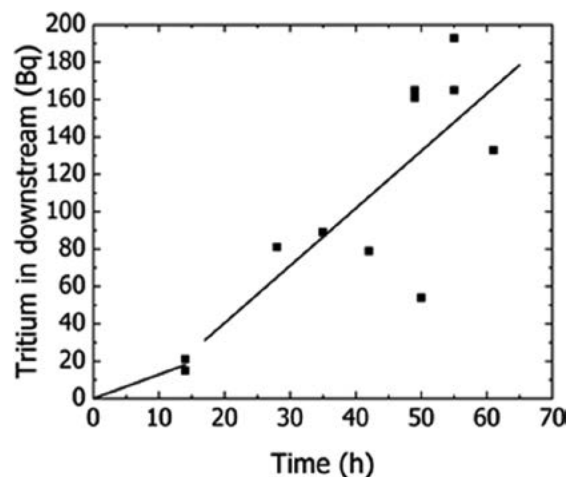


Fig. 2 Change in T permeation with elapse of time.

Other experimental studies performed in the Hydrogen Isotope Research Center in the fiscal year 2021 are the following:

- *Nano-fiber formation on tungsten alloy by helium plasma irradiation* (Y. Ueda, Osaka U.);
- *High temperature and high flux irradiation effect on hydrogen isotope retention in damaged W* (Y. Oya, Shizuoka U.);
- *Effective tritium removal under vacuum conditions* (N. Ashikawa, NIFS);
- *Effects of heat and particles load on hydrogen isotope retention in tungsten materials* (K. Tokunaga, Kyushu U.);
- *Release behaviors of hydrogen isotopes from tungsten materials exposed to hydrogen isotope plasma* (T. Otsuka, Kindai U.);
- *Suppression of tritium permeation in metals by laser-doping of impurities* (Y. Nobuta, Hokkaido U.);
- *Measurement of transmission of polymer for liquid DT for developments of laser fusion DT fuel* (Y. Arikawa, Osaka U.); and
- *Fabrication of tritium target for 14 MeV neutron irradiation experiments* (M. Kobayashi, NIFS).